High-Pressure Effects in Pyrene Crystals: Vibrational Spectroscopy

3 AUTHORS, INCLUDING:

Baozhou Sun
Washington University in St. Louis
56 PUBLICATIONS **224** CITATIONS

SEE PROFILE

Zbigniew Dreger
Washington State University
124 PUBLICATIONS **1,126** CITATIONS

SEE PROFILE

High-Pressure Effects in Pyrene Crystals: Vibrational Spectroscopy

B. Sun, Z. A. Dreger,* and Y. M. Gupta

Institute for Shock Physics and Department of Physics, Washington State University, Pullman, Washington 99164-2816

Received: July 19, 2008; Revised Manuscript Received: August 25, 2008

The response of pyrene crystals to high pressure was examined using Raman and FTIR spectroscopies. Raman spectra of external and internal modes were measured up to 11 GPa. Changes in the external modes were observed at ∼0.3 GPa, indicating the onset of a phase transition. We demonstrated that at this pressure pyrene I ($P2_1/a$, 4 mol/unit cell) transforms to pyrene III ($P2_1/a$, 2 mol/unit cell). Further increase of pressure produced a gradual broadening of the internal modes and an increase of fluorescence background, indicating the formation of another phase above 2.0 GPa. Irreversible chemical changes were observed upon gradual compression to 40 GPa. FTIR spectroscopy of the recovered product indicated a transformation of pyrene into an amorphous hydrogenated carbon (a-C:H) structure.

I. Introduction

Polycyclic aromatic hydrocarbons (PAHs) have long attracted interest as potential materials for various electronic, optoelectronic, and optical applications.[1−3] In addition to application-oriented research, significant efforts have been directed toward understanding fundamental processes related to structure−property relationships. For example, the electronic and excitonic processes in aromatic crystals have been strongly linked to both the number of aromatic rings in the molecular structure and the arrangement of molecules in the crystal.[1,2] The latter can be conveniently studied by application of external pressure.

In molecular crystals, small variations in the applied forces typically result in large changes in intermolecular separations, which can trigger dramatic reorganizations of crystal packing. Furthermore, the application of suitable pressure to unsaturated compounds, like aromatic molecules, can completely alter the bond scheme and result in transformation to a different material. Very often these transformations are not reversible and the reaction products can be recovered. These solid-state reactions have attracted great interest, and simple systems have been investigated to characterize the foundations of this new chemistry.[4,5]

Vibrational spectroscopy under high pressure provides a useful method to examine and understand the effects of polymorphic transitions and chemical transformations in molecular crystals. Here, we use vibrational spectroscopy to study the effect of pressure on pyrene crystals ($C_{16}H_{10}$), a representative of PAHs, to further our understanding of pressure-induced structural and chemical processes in aromatic molecular crystals.

At ambient conditions, pyrene crystallizes into a monoclinic structure with the $P2_1/a$ (C_{2h}^5) space group.[6,7] The unit cell contains four molecules, which maintain D_{2h} molecular symmetry in the crystal environment. The packing of the pyrene molecules in the crystal is unusual: the lattice sites are occupied by molecular pairs with a dimer structure. The adjacent parallel molecules of the dimers are relatively closely spaced, with a separation distance of 3.53 Å. This configuration causes considerable overlap of the molecular π orbitals and, conse-

quently, large intermolecular interactions. When the crystal is electronically excited, these strongly coupled pairs of molecules give rise to excimer fluorescence. Because of this property, pyrene has been an excellent model for studying excimer processes in molecular crystals.[8,9] Furthermore, because of the molecular dimeric structure, the pyrene crystal provides an attractive molecular arrangement for examining high-pressure structural and chemical stability in aromatic crystals.

There are few reports on structural changes of pyrene under high pressure. In general, previous studies were limited to a relatively small pressure range. A high pressure phase was observed at 0.26 GPa using volumetric measurements.[10] IR studies indicated a transition at 0.3 GPa.[11] Previous Raman spectroscopy measurements of external modes showed that pyrene undergoes a phase transition at ∼0.4 GPa from pyrene I (ambient phase) to pyrene II. [12] It was suggested that pyrene II has the same structure as the low-temperature phase (below ∼110 K); that is, $P2_1/a$, 4 mol/unit cell. [12−14] However, recently a different high pressure phase, namely pyrene III, was observed in the same pressure range (0.3−0.5 GPa) when pyrene was recrystallized under high pressure from a concentrated solution in dichloromethane.[15] Using X-ray diffraction, the structure of pyrene III was determined to be $P2_1/a$ with 2 mol/unit cell.[15] This inconsistency has not been addressed yet.

In contrast to the work on high-pressure polymorphism, there have no been previous studies of high-pressure chemical reactivity in pyrene crystals. However, several studies were reported on high-pressure reactivity of other aromatic compounds and various products were proposed.[5,16−26] For example, irreversible transformation was observed for polycrystalline anthracene[17] and pentacene[18,19] and was explained in terms of cross-linking between neighboring molecules, similarly to the formation of a Diels−Alder product.[18] The most extensive studies were performed on benzene, a prototype aromatic compound. Several alternative products were proposed, including bimolecular cross-linking[20] and disordered highly branched polymeric units.[21−23,25] Recently, it was shown that benzene transforms to an amorphous hydrogenated carbon structure when compressed up to 50 GPa.[24−26] In distinction to other aromatic systems, pyrene provides an attractive arrangement of molecules

---

* To whom correspondence should be addressed. E-mail: dreger@wsu.edu.

Vibrational Spectroscopy

J. Phys. Chem. A, Vol. 112, No. 42, 2008 **10547**

(dimeric pairs) to examine the pressure-associated reactivity in aromatic hydrocarbons.

The purpose of this study was to use vibrational spectroscopy: (i) to examine further the high pressure polymorphism of pyrene crystals, studying both the internal and external vibrational modes, (ii) to address the previous inconsistencies regarding the phase transition at ~0.3−0.4 GPa, and (iii) to explore the high-pressure chemical reactivity of pyrene crystals to determine the reactivity threshold and to identify the reaction product.

The reminder of the paper is organized as follows: Experimental procedures, including sample preparation and high-pressure Raman and FTIR measurements, are briefly described in the next section. Section III presents experimental data and discussion of the high-pressure polymorphism and reactivity of pyrene crystal. The main findings of this work are summarized in Section IV.

II. Experimental Methods

Pyrene of 99+% purity was purchased from Sigma-Aldrich. Single crystals of pyrene were grown from benzene solution by slow evaporation of the solvent. Pyrene crystals were also grown under high pressure in a diamond anvil cell (DAC) from dichloromethane solution.[15]

Static high pressure was generated in a modified Merrill-Bassett type DAC with 0.5 mm diamond culets. A stainless steel gasket with a 0.2 mm hole was used for the sample compartment. Cryogenically loaded argon was employed as a pressure transmitting medium. A small ruby chip was loaded with each sample to determine the pressure by measuring the wavelength shift of the ruby R_1 fluorescence line. On the basis of monitoring the separation and widths of both R_1 and R_2 lines, we confirmed that argon remained hydrostatic throughout these experiments. The pressure in the DAC was monitored with an estimated accuracy of 0.05 GPa.

Raman spectra were obtained with a Jobin Yvon T64000 micro-Raman spectrometer. The excitation wavelength was 630 nm from a Coherent dye laser pumped by an argon-ion laser. The use of this wavelength as the excitation source led to a considerable reduction in the pressure-induced luminescence background from the compressed pyrene crystal. An Olympus microscope was used to focus the laser beam to size of ~10 μm on the sample. The power at the sample was kept below 20 mW to avoid sample damage. The spectral resolution of the Raman system was better than 1 cm^{-1}.[27] The Raman spectra were analyzed with the Peakfit software using a combination of Gaussian and Lorentzian functions.

IR absorption spectra were obtained using a Fourier-transform infrared (FTIR) spectrometer (Bomem DA8) with a liquid nitrogen cooled mercury cadmium telluride (MCT) detector.[28] The instrumental resolution was about 4 cm^{-1}, and the spectra were averaged over 2000 scans. The FTIR spectra were corrected for absorption of the empty DAC with the same gasket. Both the FTIR and the Raman experiments were performed at room temperature.

III. Results and Discussion

III. A. Pressure Effects on External Modes. For a pyrene crystal group, theory predicts 12 Raman active external modes divided as follows: $\Gamma_{ext} = 6A_g + 6B_g$.[29] The external modes observed in our experiments are listed in Table 1 and compared with earlier experimental data.[12,29] In contrast to previous studies, we observed almost all of the external modes. In particular, we observed the lowest frequency mode at 18 cm^{-1} and resolved the overlapped modes at 30.1 cm^{-1} and 32.7 cm^{-1}. Furthermore,

TABLE 1: Pressure Effect on External Raman Modes of Pyrene Crystal

| mode	freq. (cm^{-1}) (this work)[a]	freq. (cm^{-1}) (ref 12)	freq. (cm^{-1}) (ref 29)	dν/dP cm^{-1} GPa^{-1b} ($\pm$0.5)	
				phase I	phase III
L_1	18.8	17.2		5.0	
L_2	30.1	29.5	30	21	6.1, 1.0
L_3	32.7			18	5.5, 2.0
L_4	41.8	40.0	41	18	
L_5	56.8	55.8	56	27	
L_6	68.3	68.3	67	30	10, 2.3
L_7	78.0	77.6	77	37	12, 2.2
L_8	94.6	95.4	92	38	15, 3.3
L_9	127.5	125.7	127	18	14.4, 3.2
L_{10}	167.0		169	17	
L_{11}	170.7		170	23	

[a] Frequencies were measured at ambient pressure. [b] The pressure dependencies of the Raman shift (dν/dP, pressure coefficient) were obtained from least-squares fits of the experimental data to either a linear or a polynomial equation.

the modes at 168 and 170 cm^{-1} were assigned to external modes in our study for reasons discussed later in this section.

The effect of pressure on the external modes was measured up to ~11 GPa using Raman spectroscopy. Because the Raman spectra above 11 GPa were significantly obscured by an increase of the luminescence background, measurements beyond this pressure were not pursued. Typical Raman spectra of external modes at several pressures are shown in part a of Figure 1. Initially all modes shifted toward higher frequencies with increasing pressure. However, above 0.3 GPa, several new features were observed in the spectra (part b of Figure 1), including: (i) discontinuities in Raman shift of some modes and (ii) decrease in a number of external modes. The modes L_1, L_4, L_5, L_{10}, and L_{11} disappeared from the spectrum, and, thus, the number of external modes above 0.3 GPa was reduced to six. Further increase of pressure up to ~11 GPa maintained the same number of peaks in the spectra but with the peaks shifted toward higher frequencies. Subsequently, a gradual decrease of pressure reproduced quite well the shape of spectra obtained during the increase of pressure with the exception of the low pressure range. In this range, the reduced number of Raman modes was observed in the spectra even below 0.3 GPa. However, the spectrum regained the original shape upon full release of pressure (part a of Figure 1).

As mentioned above, the modes located at 168 cm^{-1} (L_{10}) and 170 cm^{-1} (L_{11}) were assigned as external modes in this study. The assignment was mainly based on the pressure dependence of these modes. The details of the pressure dependence of the L_{10} and L_{11} modes are shown in part a of Figure 1. The spectra obtained at ambient 0.3 and 0.6 GPa are enlarged in the range of 150−200 cm^{-1} for the sake of clarity. It is apparent that these two modes disappear above 0.3 GPa, as do some of the other external modes. Also, the pressure coefficients of Raman shifts for these modes are similar to other external modes, which are much larger than those of the internal modes (compare Tables 1 and 2). In addition, it was previously reported that the L_{10} and L_{11} modes disappeared when pyrene was dissolved in organic solvent,[30] which further supports our assignment.

III.B. Pressure Effect on Internal Modes. For pyrene molecules, group theory predicts 36 Raman active internal modes divided as follows: $\Gamma_{int} = 13A_g + 4B_{1g} + 7B_{2g} + 12B_{3g}$.[29] Some of these modes did not have sufficient intensity to be detected in our experiments. For example, scattering from the CH stretching modes located between 3000 and 3100 cm^{-1} was too weak using 630 nm wavelength excitation and they were
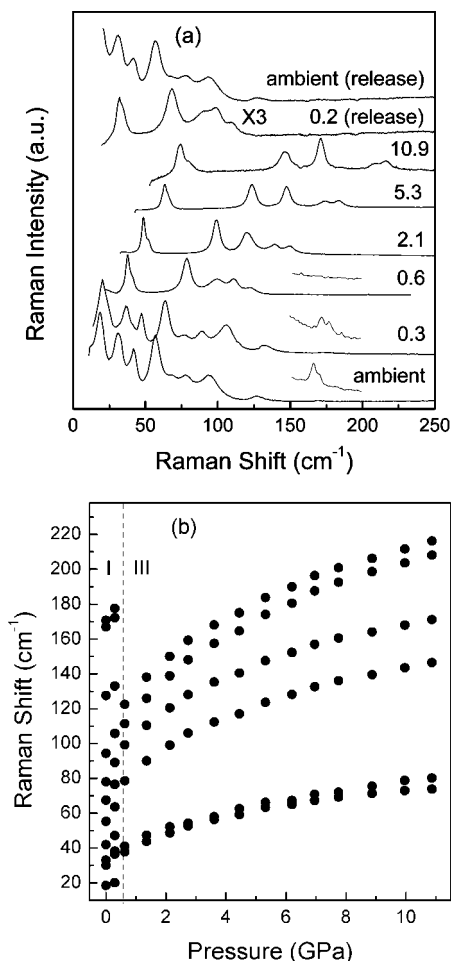
Figure 1. Pressure effect on external modes of pyrene crystal. (a) Raman spectra. Pressure values are shown in GPa next to each spectrum. Several spectra are enlarged in the range of 150−200 cm⁻¹ for clarification of the modes evolution at 168 and 170 cm⁻¹. (b) Frequency shifts of Raman modes. The vertical dashed line marks the onset of discontinuities. The Roman numbers label different pyrene polymorphs.

TABLE 2: Pressure Effect on Selected Internal Raman Modes of Pyrene Crystal

| freq. (cm⁻¹) (This work)[a]	freq. (cm⁻¹) (ref 29)	symmetry (refs 29 and 32)	$d\nu/dP$ cm⁻¹ GPa⁻¹[b] (±0.5)
262	263	B_{1g}	
266		?	
408	408	A_g	3.5, 0.8
458	458	B_{3g}	2.5, 0.6
499	498	?	2.8, 0.7
503		B_{3g}	
505	505	B_{3g}	6.0, 1.1
593	593	A_g	5.7, 1.8
712	714	?	
842	844	B_{1g}	
1108	1109	B_{3g}	2.5
1143	1144	A_g	3.1
1238	1238	B_{3g}	5.4, 1.9
1242	1243	A_g	6.1, 2.8
1405	1405	?	3.4; 2.8
1407	1408	A_g	6.8, 3.0
1594	1596	B_{3g}	6.4, 2.0
1597		B_{3g}	5.8, 2.1
1628	1630	A_g	4.4
1644	1644	A_g	4.4, 1.9

[a] Frequencies were measured at ambient pressure. [b] The pressure dependencies of the Raman shift ($d\nu/dP$, pressure coefficient) were obtained from least-squares fits of the experimental data to either a linear or a polynomial equation.

not examined in this work. All Raman internal modes observed in our study are listed in Table 2. Generally, the ambient pressure Raman spectra for the internal modes agree well with those reported previously.[29,32] The modes at 266, 503, and 1597 cm⁻¹ were not measured before[29] probably due to their low intensity. The assignments for the internal modes were adopted from ref 29.

The effect of pressure on the Raman spectra of internal modes was measured up to 10 GPa. Figure 2 shows typical Raman spectra for internal modes at several pressures in the frequency range from 400 cm⁻¹ to 1700 cm⁻¹, and Figure 3 shows the pressure dependence of the Raman shifts for selected modes. With increasing pressure, all modes shift gradually toward higher frequencies. The pressure-induced frequency shifts for internal modes are in the range of 2.5−7.0 cm⁻¹/GPa at ambient pressure and decrease to 0.7−4.0 cm⁻¹/GPa at 10 GPa. Overall, the internal modes have smaller frequency shifts compared to external modes. In addition, no apparent discontinuity, disappearance, or splitting was observed for the internal modes in the pressure range examined, in contrast to the external modes. However, some internal modes showed considerable broadening above ∼2 GPa. The effect of pressure on the full width at half-maximum (fwhm) for selected internal modes is presented in Figure 4. One possible source of the line width broadening in

the high-pressure experiments is a pressure gradient in the sample due to nonhydrostaticity of the medium. The pressure gradient would mean that the molecules would experience slightly different pressures depending on their location within the pressure cell. As can be seen in Figure 4, the broadening extent and evolution with pressure differ among various modes. This implies that the increase in linewidths is mostly due to a distribution in distortions of different bonds in the molecules. However, we cannot exclude the contribution to broadening of Raman modes at higher pressures from the non-hydrostaticity. Note that non-hydrostaticity can be present despite the lack of broadening in the ruby lines.

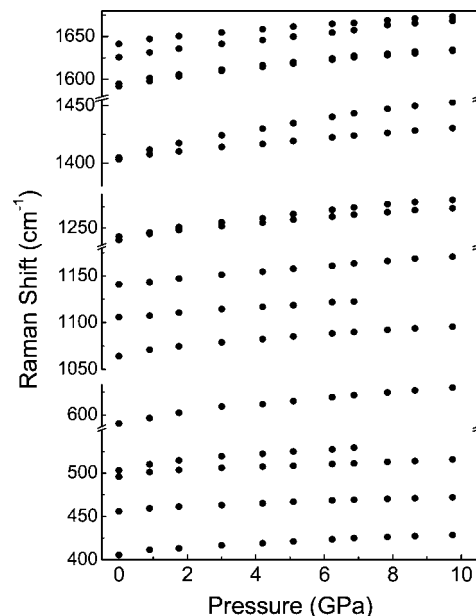**III.C. High-Pressure Polymorphism of Pyrene Crystal.** The studies of external and internal Raman modes under pressure indicated two instances of Raman spectra changes: (i) discontinuities in pressure shift and reduction in the number of external modes above ∼0.3 GPa and (ii) increase in the line width of some internal modes above ∼2 GPa. The reduction in the number of external modes without changes in the internal modes above 0.3 GPa would indicate a decrease in the number of molecules in the unit cell. Furthermore, the decrease of external modes from 11 to 6 would imply the reduction of molecules in the unit cell from 4 to 2. This proposal is in clear contrast with the previous suggestion that the structure for pyrene above ∼0.4 GPa is similar to the low temperature structure[12] because the low temperature structure was determined to be $P2_1/a$ with 4 mol/unit cell (pyrene II).[14]

On the other hand, Fabbiani et al.[15] recently reported another structure for pyrene crystals above ∼0.3 GPa where the pyrene crystals were grown from dichloromethane solution under high-pressure in the DAC. The structure of those crystals were determined by X-ray diffraction as $P2_1/a$ with 2 mol/unit cell (pyrene III), which is the same number of molecules that we propose from our measurements. To explore further a possible similarity between the high-pressure structure of pyrene observed in this study and pyrene III, we performed Raman measurements on pyrene III. For this purpose, we grew a single
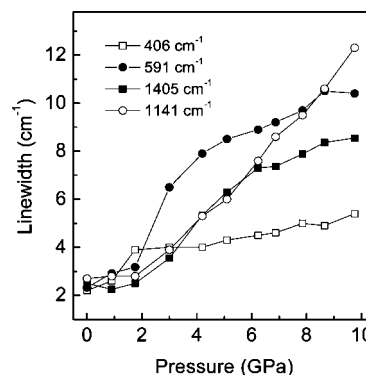
Vibrational Spectroscopy

J. Phys. Chem. A, Vol. 112, No. 42, 2008 **10549**
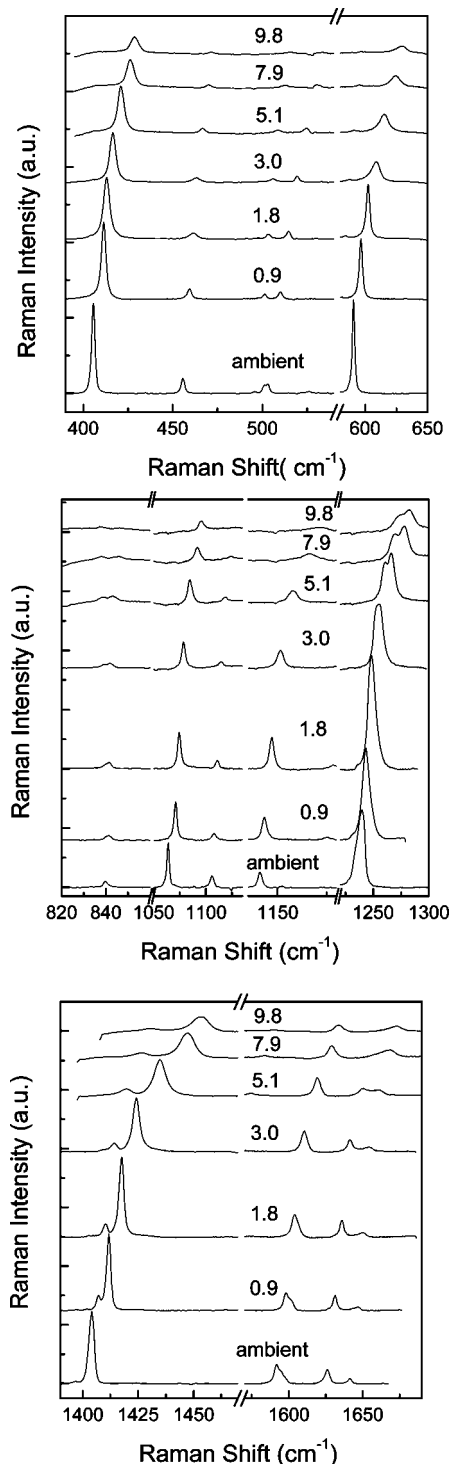
Figure 2. Raman spectra of internal modes of pyrene crystal in the frequency range of 400−1700 cm⁻¹ at several pressures. Pressure values are shown in GPa next to each spectrum.

Figure 3. Frequency shifts of internal modes of pyrene crystal as a function of pressure.
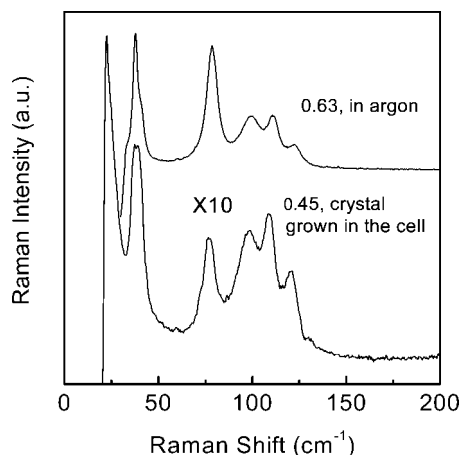

Figure 4. Pressure effect on the line width of selected internal modes of pyrene crystal.

It should be mentioned that the observed line width broadening of the internal modes above 2 GPa was accompanied by an increase in the luminescence background. The line width broadening was fully reversible upon release of pressure but the Raman spectra of released crystals still showed the increased luminescence background. Because we use 630 nm excitation for our Raman measurements, which is far from the electronic transition for the pyrene crystal (absorption edge above 3 eV (∼415 nm)),[33] the observed luminescence background likely originates from excited structural defects. These defects could be formed during the phase transition at ∼0.3 GPa and also above 2 GPa. We believe that the line broadening above 2 GPa could be caused by some type of second-order phase transition. On the basis of IR spectra, it was previously suggested that pyrene can undergo another phase transition between 3.0 and 4.5 GPa.[11]

III. D. High-Pressure Induced Chemical Reaction. As mentioned above, the Raman measurements could not be performed beyond ∼11 GPa because of the increased luminescence background. However, we followed the changes in the sample color with increasing pressure. The color of the pyrene crystal changed from colorless at ambient pressure to deep red at ∼25 GPa and to black at ∼40 GPa (also pictures in Figure 6). The change of color was irreversible upon release of the sample to ambient pressure. The recovered product (RP) from

crystal of pyrene from a concentrated solution of pyrene in dichloromethane under pressure in a DAC. The Raman spectrum of this crystal is compared, in Figure 5, with the Raman spectrum of a pyrene crystal compressed to 0.6 GPa in the argon pressure medium. One can notice a close similarity between the two spectra with respect to the number and position of the peaks. This result indicates that above 0.3 GPa, pyrene crystal assumes the structure of pyrene III rather than the pyrene II structure. The difference between our finding and the previously suggested structure is under investigation.[31]

Figure 5. Raman spectra of pyrene crystal. Top: 0.63 GPa, argon used as pressure transmitting medium. Bottom: 0.45 GPa, pyrene crystal grown in DAC from pyrene dissolved in dichloromethane. The intensity of Raman spectrum is multiplied by 10. Note that some difference in position of peaks in two spectra results from the difference in pressures in these two experiments.

~40 GPa was insoluble in many organic solvents, for example, benzene, dichloromethane, methanol, and acetone, indicating the formation of higher molecular weight compound. To characterize the RP, we first used Raman spectroscopy. However, the Raman spectra did not show any peaks, likely due to the highly disordered nature of the recovered samples and the large luminescence background. Therefore, FTIR spectroscopy was used to obtain information on possible structures of the recovered product.

The FTIR spectra of the products recovered from compression to 25 and 40 GPa are presented among other spectra in Figure 6. Spectrum (a) in this figure represents the IR spectrum of fresh, untreated pyrene crystal. More than 20 peaks were observed in the $600-1700$ cm^{-1} range with good agreement with previous studies.[34–36] Because of diamond absorption, spectra in the range of $1800-2700$ cm^{-1} were not examined. The peak at 3040 cm^{-1}

(labeled with number 1) corresponds to C−H stretching vibrations with sp^2 hybridized carbon atom (sp^2CH).[37] Additional peaks on both sides of the 3040 cm^{-1} absorption band were found to be the interference fringes from the thin sample. Spectrum (b) in Figure 6 was measured on the sample recovered from compression to 25 GPa. This spectrum had fewer peaks than the spectrum of untreated pyrene. Also, some peaks had much lower intensity. However, the most important change in the spectrum occurs on the low frequency side of the C−H stretching mode, located at 3040 cm^{-1}, labeled as 1. Two weak bands emerged at 2861 and 2916 cm^{-1}, labeled as 3 and 2, respectively. These bands could be assigned to the C−H symmetric and antisymmetric stretching vibrations corresponding to the sp^3 hybridized carbon atom.[37] Furthermore, the peak at 2861 cm^{-1} could correspond to the sp^3CH$_3$ configuration and the peak at 2916 cm^{-1} the sp^3CH configuration.[37] Spectrum (c) in Figure 6 was measured using the sample recovered from compression to 40 GPa. This spectrum has only a few, residual pyrene peaks corresponding to CH$_2$ rocking (710 cm^{-1}, 748 cm^{-1}), CH$_2$ wagging (963 cm^{-1}), C=C stretching (1599 cm^{-1}), and CH stretching with the sp^2 carbon atom (3040 cm^{-1}).[37] All other bands can be attributed to the recovered product and are quite broad as would be expected for a disordered compound. In particular, the broad bands between 1100 and 1600 cm^{-1} can be characteristic of a highly branched structure of recovered product.[37] It should be noticed that some interference fringes are superimposed to the spectral profile in the range of $1100-1600$ cm^{-1} due to the thin sample. Furthermore, the peaks at 2861 and 2916 cm^{-1} are stronger and the peak at 3040 cm^{-1} is weaker compared to the spectrum for sample recovered from 25 GPa. The decrease in intensity of peak 1, and increase in intensity of peaks 2 and 3 indicates that more unsaturated carbon atoms (sp^2-type) were converted into saturated carbon (sp^3-type) upon compression to 40 GPa than compression to 25 GPa. The above observations are quite similar to those observed in compressed benzene, for which the transformation to an amorphous hydrogenated carbon structure (*a*-C:H) was proposed.[25,26]
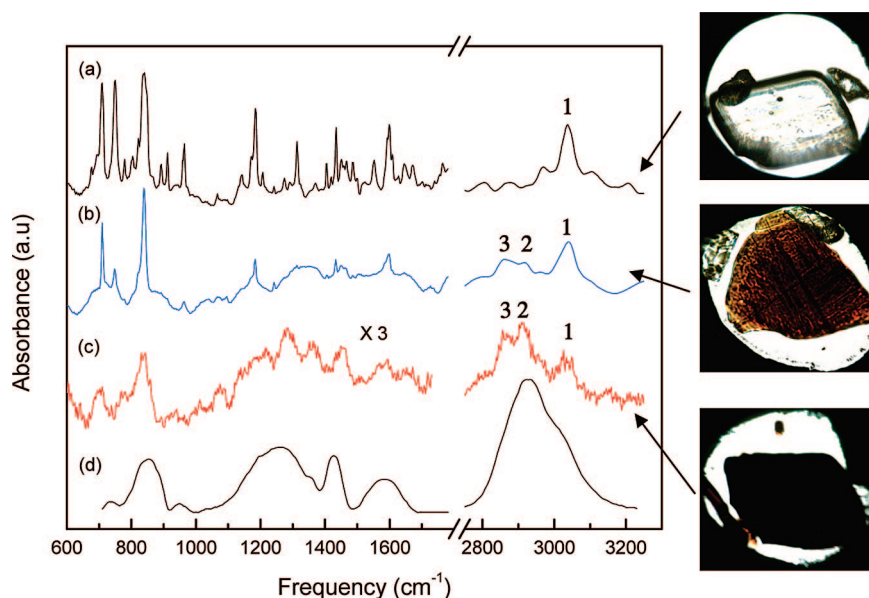
Figure 6. FTIR spectra at ambient pressure. (a) pyrene crystal untreated (no previous compression), (b) recovered product after compression to ~25 GPa, (c) recovered product after compression to 40 GPa, (d) *a*-C:H from ref 37 (spectrum was rescaled to make it comparable to our spectra of recovered product). Label 1 designates the CH stretching vibration with sp^2 hybridized carbon atom; labels 2 and 3 designate, respectively, the CH stretching symmetric and antisymmetric vibrations with sp^3 hybridized carbon atom. Images shown next to each spectrum were taken in a diamond anvil cell at ambient pressures, in three separate experiments.

Vibrational Spectroscopy

J. Phys. Chem. A, Vol. 112, No. 42, 2008 **10551**

Therefore, the IR spectra of the recovered product were further compared with IR spectrum of an *a*-C:H compound.[25,37] This compound was obtained from the chemical vapor deposition (CVD) of benzene.[37] Spectrum (d) in Figure 6 represents the IR absorbance of the CVD sample, rescaled for an easier comparison with the other spectra. Despite the low intensity and interference peaks in the spectrum of the recovered product (spectrum (c)), one can notice a qualitative similarity between the spectra (c) and (d). In particular, both spectra show characteristic broad bands around 830, 1250, 1420, 1590, 2900, and 3000 cm^{-1}. The similarity between the IR spectra of the recovered high pressure product from 40 GPa and the *a*-C:H compound suggests that pyrene was converted to an amorphous hydrogenated carbon structure, similar to that found for benzene under high pressure.[25] We also note that some new bands (837, 2861, and 2916 cm^{-1}) in spectrum (c) are red-shifted by ~15 cm^{-1} compared to those in the *a*-C:H sample. The lower vibrational frequencies in RP may indicate a shorter olefinic chain than for the CVD sample.[38] The opposite case was observed in the recovered product from benzene.[25]

The relative amounts of sp^3 and sp^2 carbon atoms (Csp^3/Csp^2) in the hydrogenated amorphous carbon (*a*-C:H) compounds is an important parameter that can characterize the material mechanical properties.[25,37,39] Therefore, we evaluated the ratio of Csp^3/Csp^2 in the recovered product obtained from the compression of pyrene to 40 GPa. The ratio of Csp^3/Csp^2 can be related to the ratio of integrated intensity for C−H sp^3 and C−H sp^2 bands [I(C−H sp^3)/I(C−H sp^2)] in the IR spectra. For the product recovered from the compressed pyrene, the ratio of integrated intensities is ~1.7 as obtained from fitting the CH stretching vibrational bands in Figure 6 (spectrum (c)). Using a semiquantitative diagram correlating the ratio of Csp^3/Csp^2 with the ratio of I(C−H sp^3)/I(C−H sp^2) presented in ref 25, we obtain a Csp^3/Csp^2 ratio of ~1.0, that is, ~50% abundance of sp^3 carbon atoms in the sample. This value is lower than for the amorphous product recovered from benzene (76%),[25] which is consistent with the lower hydrogen/carbon ratio in pyrene ($C_{16}H_{10}$) than in benzene (C_6H_6).

IV. Summary and Conclusions

Pressure-induced structural and chemical changes in pyrene crystals were investigated using vibrational spectroscopy. We found that pyrene crystals undergo a phase transition from pyrene I ($P2_1/a$, 4 mol/unit cell) to pyrene III ($P2_1/a$, 2 mol/unit cell) above ~0.3 GPa, which is in contrast to a previous report proposing a phase transition to pyrene II ($P2_1/a$, 4 mol/unit cell). The observed phase transition was fully reversible upon release of pressure. Broadening of the internal modes above ~2 GPa indicated the possibility of another phase transition, possibly a second-order transition.

Irreversible chemical transformations were observed upon compression of pyrene crystals to 25 and 40 GPa. The high-pressure products recovered from these pressures were examined using FTIR spectroscopy. The IR spectra of the recovered products were similar to the IR spectrum of the CVD layer of an amorphous hydrogenated carbon compound (*a*-C:H). This evidence suggests that pyrene transforms to the *a*-C:H amorphous structure, similar to that observed for benzene under high pressure. The transformation of the CH bonding scheme from sp^2 to sp^3 hybridized was estimated to be ~50% in the recovered product.

References and Notes

(1) Pope, M., Swenberg; C. E. *Electronic Processes in Organic Crystals and Polymers*; Oxford University Press: New York, 1999.

(2) Silinsh, E. A.; Capek, V. *Organic Molecular Crystals: Interaction, Localization, and Transport Phenomena*; Springer-Verlag: Berlin, Heidelberg, and New York, 1994.

(3) Farchioni, R.; Grosso, G. *Organic Electronic Materials: Conjugated Polymers and Low Molecular Weight Organic Solids*; Springer: Berlin, 2001.

(4) Drickamer, H. G.; Frank, C. W. *Electronic Transitions and the High Pressure Chemistry and Physics of Solids*; Chapman and Hall: London, 1973.

(5) Schettino, V.; Bini, R. *Phys. Chem. Chem. Phys.* **2003**, *5*, 1951.

(6) Robertson, J. M.; White, J. G. *J. Chem. Soc.* **1947**, 358.

(7) Hazell, A. C.; Larsen, F. K.; Lehmann, M. S. *Acta Crystallogr. B* **1972**, *28*, 2977.

(8) Birks, J. B. *Photophysics of Aromatic Molecules*; New York, London, 1970.

(9) Birks, J. B. *Rep. Prog. Phys.* **1975**, *38*, 903.

(10) Vaidya, S. N.; Kennedy, G. C. *J. Chem. Phys.* **1971**, *55*, 987.

(11) Hamann, S. D. *High Temp. High Press.* **1978**, *10*, 503.

(12) Zallen, R.; Griffiths, C. H.; Slade, M. L. *Chem. Phys. Lett.* **1976**, *39*, 85.

(13) Knight, K. S., Shankland, K. , Shankland, N. *Acta Crystallogr. A*, 1999; *55*, Supplement, Abstr. M07.EE.004.

(14) Frampton, C. S.; Knight, K. S.; Shankland, N.; Shankland, K. *J. Mol. Struct.* **2000**, *520*, 29.

(15) Fabbiani, F. P. A.; Allan, D. R.; Parsons, S.; Pulham, C. R. *Acta Crystallogr. B* **2006**, *62*, 826.

(16) Because this work concerns the study under static compression and at room temperature, the references are only related to previous work under static compression.

(17) Murphy, R. B.; Libby, W. F. *J. Am. Chem. Soc.* **1977**, *99*, 39.

(18) Drickamer, H. G. *Science* **1967**, *156*, 1183.

(19) Aust, R. B.; Drickamer, H. G. *J. Chem. Phys.* **1964**, *41*, 1856.

(20) Pucci, R.; March, N. H. *J. Chem. Phys.* **1981**, *74*, 1373.

(21) Pruzan, Ph.; Chervin, J. C.; Thiery, M. M.; Itie, J. P.; Besson, J. M. *J. Chem. Phys.* **1990**, *92*, 6910.

(22) Gauthier, M.; Chervin, J. C.; Petitet, J. P. In *Frontiers of High Pressure Research*; Hochheimer, H. D., Etters, R. D., Eds.; Plenum: New York, 1991; p 87.

(23) Thiery, M. M.; Besson, J. M.; Bribes, J. L. *J. Chem. Phys.* **1992**, *96*, 2633.

(24) Ciabini, L.; Santoro, M.; Gorelli, F. A.; Bini, R.; Schettino, V.; Raugei, S. *Nature Mater.* **2006**, *6*, 39.

(25) Ciabini, L.; Santoro, M.; Bini, R.; Schettino, V. *J. Chem. Phys.* **2002**, *116*, 2928.

(26) Ciabini, L.; Santoro, M.; Bini, R.; Schettino, V. *Phys. Rev. Lett.* **2002**, *88*, 085505.

(27) Dreger, Z. A.; Gupta, Y. M. *J. Phys. Chem. B* **2007**, *111*, 3893.

(28) Zhuravlev, K. K.; McCluskey, M. D. *J. Chem. Phys.* **2002**, *117*, 3748.

(29) Bree, A.; Kydd, R. A.; Mira, T. N.; Vilkoss, V. V. B. *Spectrochim. Acta*, **1971**, *27A*, 2315.

(30) Lyrra, M.; Ränsänen, J.; Stenman, F. *Physica Fennica* **1975**, *10*, 191.

(31) Sun, B.; Dreger, Z. A.; Gupta, Y. M., to be published.

(32) Shinohara, H.; Yamakita, Y.; Ohno, K. *J. Mol. Struct.* **1998**, *442*, 221.

(33) Takahashi, N.; Gombojav, B.; Yoshinari, T.; Nagasaka, S.; Takahashi, Y.; Yamamoto, A.; Goto, T.; Kasuya, A. *J. Sol. State Chem.* **2004**, *177*, 3479.

(34) Califano, S.; Abbondanza, G. *J. Chem. Phys.* **1963**, *39*, 1016.

(35) Langhoff, S. R. *J. Phys. Chem.* **1996**, *100*, 2819.

(36) Vala, M.; Szczepanski, J.; Pauzat, F.; Parsisel, O.; Talbi, D.; Ellinger, Y. *J. Phys. Chem.* **1994**, *98*, 9187.

(37) (a) Dischler, B.; Bubenzer, A.; Koidl, P. *Solid State Commun.* **1983**, *48*, 105. (b) Dischler, B.; Bubenzer, A.; Koidl, P. *Appl. Phys. Lett* **1983**, *42*, 636.

(38) (a) Snyder, R. G.; Schachtschneider, J. H. *Spectrochim. Acta* **1963**, *19*, 85. (b) Schachtschneider, J. H.; Snyder, R. G. *Spectrochim. Acta* **1963**, *19*, 117.

(39) Tsai, T. *Mater. Sci. Forum*, **1990**, *71*, 52–53.